arXiv:2506.15681v3 [cs.CL] 2 Mar 2026

GenRecal: Generation after Recalibration from Large to Small Vision-Language Models

Byung-Kwan Lee[1], Ryo Hachiuma[1], Yong Man Ro[2],
Yu-Chiang Frank Wang[1,3], and Yueh-Hua Wu[1]

[1] NVIDIA
[2] KAIST
[3] National Taiwan University

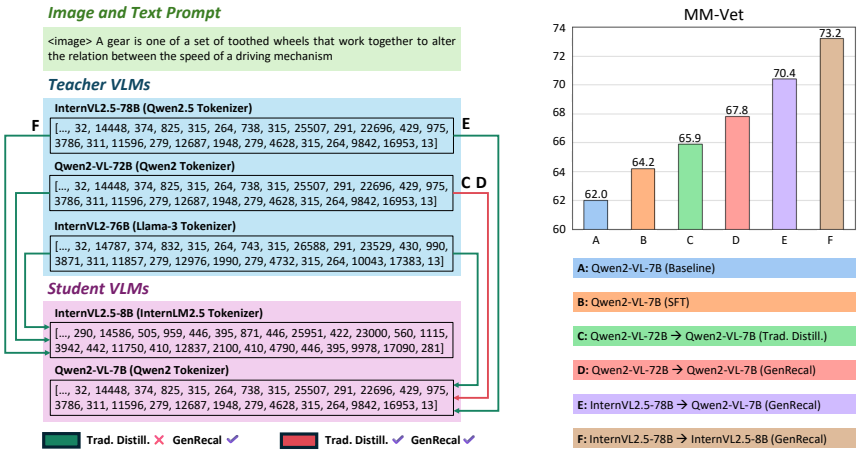

Fig. 1: (Left) Visualizing the token indices of a given image and text prompt and representing the possibility of distillation among various VLM pair combinations, comparing traditional distillation with our proposed distillation framework, GenRecal. Note that the parentheses mean each VLM's LLM tokenizer, '...' indicates the placement of image features, and the number of these features varies depending on the image embedding strategy. (Right) Comparing the performance of a challenging evaluation benchmark, MM-Vet [115], with [A] baseline, [B] SFT on the baseline, [C] traditional distillation and [D] GenRecal from same token types of large VLMs, and GenRecal with more powerful [E] large and [F] small VLMs.

Abstract. Recent advancements in vision-language models (VLMs) have leveraged large language models (LLMs) to achieve performance on par with closed-source systems like GPT-4V. However, deploying these models in real-world scenarios, particularly on resource-constrained devices, remains challenging due to their substantial computational demands. This has spurred interest in distilling knowledge from large VLMs into smaller, more efficient counterparts. A key challenge arises here from the diversity of VLM architectures, which are built on different LLMs and employ varying token types—differing in vocabulary size, token splits, and token index ordering. To address this challenge of limitation to a specific VLM type, we present **Gen**eration after **Recal**ibration (GenRecal), a general-purpose distillation framework for VLMs. GenRecal

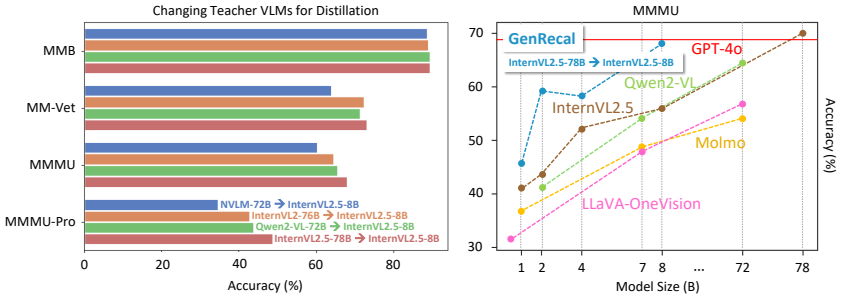

Fig. 2: (Left) Comparison of the challenging benchmark performances, MMB [64], MM-Vet [115], MMMU [117], and MMMU-Pro [118] by changing large VLMs. The more powerful large VLMs we select, the greater the performance improvement we can achieve. (Right) Comparing the performance of the challenging benchmark: MMMU [117], with GenRecal and various VLMs across model sizes. Note that all the experiments in Fig. 1 and Fig. 2 are conducted on the equal training dataset.

incorporates a Recalibrator that aligns and adapts feature representations between heterogeneous VLMs, enabling effective knowledge transfer across different types of VLMs. Through extensive experiments on multiple challenging benchmarks, we demonstrate that GenRecal significantly improves baseline performances, eventually outperforming large-scale open- and closed-source VLMs.

Keywords: Cross-Tokenizer · Model Distillation · Efficient AI

1 Introduction

Vision-language models (VLMs) have emerged as powerful tools for understanding and processing multimodal information, enabling tasks such as image captioning and visual question answering [56,93]. Recent advancements in VLMs [3, 55,61] have leveraged large-scale language models (LLMs) to enhance reasoning and generation capabilities by incorporating extensive textual knowledge [79,88]. In pursuit of superior performance, state-of-the-art VLMs [20,26,28,53,105] now integrate scaled-up LLMs such as 72B model parameters, achieving results comparable to proprietary models like GPT-4V [74] and Claude-3.5 Sonnet [4].

However, the increasing scale of recent VLMs introduces substantial computational overhead, limiting their practicality in real-world scenarios—particularly for on-device deployment. To mitigate this challenge, recent work has explored distillation techniques [11, 31, 86] that transfer knowledge from large (teacher) VLMs to smaller (student) ones. Yet, existing distillation methods suffer from a fundamental limitation: they typically assume that teacher and student produce sequences of equal token length, enabling token-level distance metrics such as KL divergence. This assumption breaks down when the two models use different tokenizers or adopt different image-splitting mechanisms (see Appendix A), making the distillation process infeasible. Consequently, the range of viable teacher–student VLM pairs becomes severely restricted (see Appendix B). In other words, current distillation approaches only operate when the teacher and

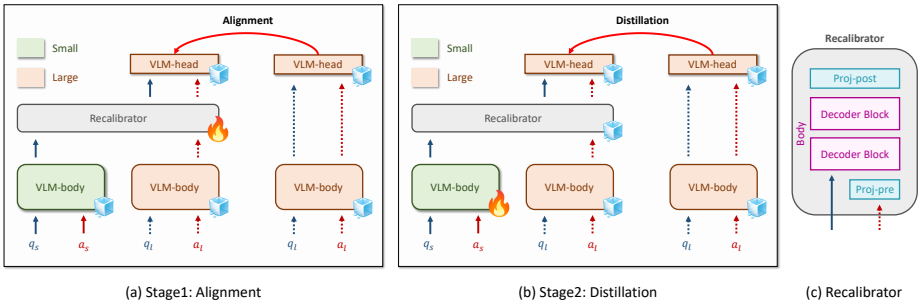

Fig. 3: Overview of the GenRecal architecture and its training stages. We denote the question and answer tokens from the small VLM as q_s and a_s, and those from the large VLM as q_l and a_l. For simplicity, the vision encoder and image-token projector are omitted from the illustration. Note that Recalibrator is used only during training as a bridge between heterogeneous VLMs. During inference, Recalibrator is removed, leaving the small VLM's architecture unchanged and no extra computational cost.

student share identical vocabulary sizes, token split, and token index ordering schemes (referred to as token types), as illustrated on the left side of Fig. 1. These differences naturally lead to mismatched input or output token lengths across VLMs, preventing effective distillation. Note that even VLMs within the same family may employ different token types, further hindering compatibility.

To overcome this limitation, we propose **Gen**eration after **Recal**ibration (GenRecal), a general-purpose distillation framework for token types-agnostic VLM distillation. At its core, GenRecal introduces a *Recalibrator* that aligns and adapts the feature representations of small VLMs with those of large VLMs. This design is inspired by prior studies demonstrating that word embeddings from different models can be linearly mapped into a shared embedding space [24,72,87]. Unlike approaches that align only word embeddings, Recalibrator performs joint visual–linguistic alignment on the hidden representations before the language head. By projecting small VLM features into large VLMs' feature space as shared representation, Recalibrator effectively bridges the gap between the large and small VLMs, enabling general-purpose knowledge transfer.

To demonstrate the necessity of GenRecal, we first compare its performance with that of traditional distillation, as shown in experiment types C and D of Fig. 1. Although both experiments employ the same token types of VLMs—Qwen2-VL-72B as the teacher and Qwen2-VL-7B as the student—GenRecal consistently outperforms the traditional distillation method implemented by LLaVA-KD [11]. This result highlights that aligning feature representations between large and small VLMs is crucial for minimizing information loss during distillation, even when the models are homogeneous. Moreover, when we replace the large VLM from Qwen2-VL-72B with the more powerful InternVL2.5-78B, GenRecal achieves enhanced performance. Subsequently, replacing the small VLM with InternVL2.5-8B leads to an even stronger model, as summarized on the right side of Fig. 1. These experiments highlight the significance of GenRecal because traditional methods cannot handle VLM pairs with different token types.

Our contributions can be summarized as follows:

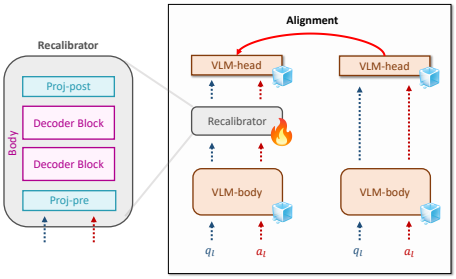

Fig. 4: Overview of regularization simultaneously done with first training stage-alignment. Note that its propagation rule is different with Fig. 3(c) where Recalibrator takes small VLM's tokens for the question and large VLM's tokens for the answer. In contrast, in this figure, only large VLM's tokens (question and answer) are fed into Recalibrator. Basically, *Rec-body* has the hidden dimension of the small VLM, so we should change this hidden dimension of large VLM's tokens to that of small VLM's ones via *Proj-pre* when the large VLM's tokens are fed into Recalibrator.

- **Token Types-agnostic Recalibration:** GenRecal employs Recalibrator to align and adapt feature representations of large and small VLMs, enabling general-purpose distillation across various token types of vocabulary size, token splits, and token index ordering.
- **Broad Applicability:** GenRecal is compatible with a wide range of VLM architectures across different model sizes, overcoming the challenge of selecting large VLMs that have different token types and demonstrating its practicality for real-world deployment in resource-constrained settings.

2 Related Work

Large-scale VLMs such as NVLM-72B [26], Qwen2-VL-72B [105], and InternVL2.5-78B [20] have closely reached the performances of GPT-4V [74] and Claude-3.5 Sonnet [4] since the evolution of VLMs (see Appendix C). However, they are imposing a significant computational burden in real-world applications, such as on-device processing. Hence, it is necessary to develop small VLMs to be embedded on the light devices, and this demand has led to the emergence of two types of distillation approaches. First one is constructing visual instruction tuning datasets [19, 33, 40, 53, 91, 106, 119, 123] from large-scale VLMs to train small VLMs with those curated datasets. Second one is conducting distillation: LLaVA-MoD [86] conducts logits-based distillation on a mixture of expert (MoE) [81, 84] architectures. LLaVA-KD [11] also uses logits-based distillation but presents three-stage training process where trainable parameters are different for each stage to effectively warm-up and distill the knowledge. Align-KD [31] distills both vision encoder features and decoder logits, while encouraging the student VLMs' first decoder layer's attention map to resemble that of the large VLM. MoVE-KD [13] employs multiple vision encoders to large VLMs and utilize a mixture of LoRA [41] to small VLM. It distills visual information of large VLMs by using a visual attention map. Besides, there are earlier distillation stud-

Algorithm 1 First stage Loss Functions (Alignment)

Input: $(q_l,\ a_l)$, $(q_s,\ a_s)$, gt_l (label index)
$[z_{q_l}, z_{a_l}] \leftarrow \textit{VLM-body}_l([q_l, a_l])$
$[z_{q_s}, z_{a_s}] \leftarrow \textit{VLM-body}_s([q_s, a_s])$
$[r_{q_s}, r_{a_l}] \leftarrow \textit{Recalibrator}([z_{q_s}, z_{a_l}])$
$\mathcal{L}_{ar} \leftarrow \mathrm{CE}(\textit{VLM-head}_l(r_{a_l}), gt_l)$
$\mathcal{L}_{kl} \leftarrow \mathcal{D}_{\mathrm{KL}}(\textit{VLM-head}_l(z_{a_l}) \mid \textit{VLM-head}_l(r_{a_l}))$
Return: $\mathcal{L}_{ar} + \mathcal{L}_{kl}$

ies (see Appendix C), but they do not consider either token-derived or different token type distillation.

However, existing works are largely constrained to VLMs sharing identical token types, including vocabulary size, token segmentation, and token index ordering. When the large and small VLMs employ different tokenizers or image embedding strategies, distillation becomes problematic—KL divergence cannot be computed due to mismatched output token counts, and token indices may no longer correspond to semantically equivalent meaning. Overcoming this limitation would represent a significant advancement, broadening the applicability and robustness of distillation techniques for diverse VLM architectures.

3 GenRecal: Generation after Recalibration

3.1 Model Architecture & Various Accommodation

We briefly illustrate the overall model architecture and training procedure in Fig. 3. GenRecal consists of three main components: a large (teacher) VLM, a small (student) VLM, and a Recalibrator module. For the large VLMs, we select models with over 72B parameters to ensure competitive performance: NVLM-72B (Qwen2-72B) [26], Qwen2-VL-72B (Qwen2-72B) [105], InternVL2-76B (Llama3-70B) [21], and InternVL2.5-78B (Qwen2.5-72B) [20]. For the small VLMs, we adopt various model sizes, including Qwen2-VL-2B/7B (Qwen2-2B/7B) and InternVL2.5-1B/2B/4B/8B (InternLM2.5-1.8B/7B and Qwen2.5-0.5B/3B/72B). Note that the parentheses denote the LLMs used within each VLM. Throughout this section, we divide a VLM architecture into four key modules: the vision encoder, vision projector, *VLM-body*, and *VLM-head* (*i.e.* language head). Recalibrator is designed to acquire shared feature representations within a common latent space. It consists of two decoder blocks and two projection layers, as depicted in Fig. 3(c). We denote the decoder blocks as *Rec-body*, and the projection layers as *Proj-pre* and *Proj-post*. The decoder blocks, *Rec-body*, adopt the same structural design as the student VLM's decoder, while both *Proj-pre* and *Proj-post* are implemented as single linear layers.

3.2 Design and Propagation of Recalibrator

To construct a shared representation space, we first extract and align hidden features from both the large and small VLMs. Since the hidden space of a large

Algorithm 2 First stage Regularization (Alignment)

Input: $(q_l,\ a_l)$, gt_l (label index)
$[z_{q_l}, z_{a_l}] \leftarrow$ *VLM-body*$_l([q_l, a_l])$
$[r_{q_l}, r_{a_l}] \leftarrow$ *Recalibrator*$([z_{q_l}, z_{a_l}])$
$\mathcal{L}_{ar} \leftarrow \mathrm{CE}(\textit{VLM-head}_l(r_{a_l}), gt_l)$
$\mathcal{L}_{kl} \leftarrow \mathcal{D}_{\mathrm{KL}}(\textit{VLM-head}_l(z_{a_l}) \mid \textit{VLM-head}_l(r_{a_l}))$
Return: $\mathcal{L}_{ar} + \mathcal{L}_{kl}$

Algorithm 3 Second stage Loss Functions (Distillation)

Input: $(q_l,\ a_l)$, $(q_s,\ a_s)$, $(gt_l,\ gt_s)$ (label index)
$[z_{q_l}, z_{a_l}] \leftarrow$ *VLM-body*$_l([q_l, a_l])$
$[z_{q_s}, z_{a_s}] \leftarrow$ *VLM-body*$_s([q_s, a_s])$
$[r_{q_s}, r_{a_l}] \leftarrow$ *Recalibrator*$([z_{q_s}, z_{a_l}])$
$\mathcal{L}_{ar} \leftarrow \mathrm{CE}(\textit{VLM-head}_l(r_{a_l}), gt_l)$
$\mathcal{L}_{ar} \leftarrow \mathcal{L}_{ar} + \mathrm{CE}(\textit{VLM-head}_s(z_{a_s}), gt_s)$
$\mathcal{L}_{kl} \leftarrow \mathcal{D}_{\mathrm{KL}}(\textit{VLM-head}_l(z_{a_l}) \mid \textit{VLM-head}_l(r_{a_l}))$
Return: $\mathcal{L}_{ar} + \mathcal{L}_{kl}$

VLM typically encompasses a richer vocabulary and more expressive representations, we regard it as the shared latent space which the small VLM is projected into. However, direct alignment of the two VLMs' tokens within this space is infeasible due to discrepancies in vocabulary size, token split, and token index ordering. To overcome this challenge, we draw inspiration from the principle of *autoregressive modeling*, wherein a model predicts answer tokens for the given question tokens.

Specifically, we feed the same question-answer pair into both the large and small VLMs, obtaining their *VLM-body* outputs as:

$$\begin{aligned} [z_{q_l}, z_{a_l}] &= \textit{VLM-body}_l([q_l, a_l]), \qquad (l : \text{large}) \\ [z_{q_s}, z_{a_s}] &= \textit{VLM-body}_s([q_s, a_s]), \qquad (l : \text{small}) \end{aligned} \tag{1}$$

where q and a denote the question and answer tokens produced by each model's vision encoder, vision projector, and word embedding [71]. We then extract the question features z_{q_s} from the small VLM and the answer features z_{a_l} from the large VLM, and concatenate them to form a joint sequence: $[z_{q_s}, z_{a_l}]$, which is then passed through Recalibrator. Because directly embedding both features into a shared space is infeasible due to different token types, we instead design an autoregressive loss that predicts the answer token index of the large VLM given the question token index of the small VLM. This loss encourages Recalibrator to effectively project the small VLM's features into the large VLM's latent space.

However, the hidden dimensions of large and small VLMs often differ. To address this, in Recalibrator, we first apply *Proj-pre* to z_{a_l}, aligning its dimensionality to that of z_{q_s}. The concatenated sequence $[z_{q_s}, \textit{Proj-pre}(z_{a_l})]$ is then propagated through *Rec-body* decoder blocks. The output of *Rec-body* is sub-

Table 1: Evaluation of standard model size open-source VLMs and GenRecal on several challenging vision-language benchmarks: AI2D [44], ChartQA [69], MathVista [66], MMB [64], MMB^{CN} [64], MM-Vet [115], MMMU [117], MMMU-Pro [118], BLINK [32], SEED-2-Plus [54], and RealWorldQA (RWQA). We use the notations of 'XX-GenRecal (YY)' where 'XX' and 'YY' denote the student (small) and teacher (large) VLM.

VLMs	AI2D	ChartQA	MathVista	MMB	MMB^{CN}	MM-Vet	MMMU	MMMU-Pro	BLINK	SEED-2-Plus	RWQA
Cambrian-1-8B [98]	73.0	73.3	49.0	75.9	-	48.0	42.7	-	44.9	59.7	60.0
Cambrian-1-13B [98]	73.6	73.8	48.0	75.7	-	48.9	40.0	-	43.1	60.0	58.6
Eagle-8B [85]	76.1	80.1	52.7	75.9	-	33.3	43.8	-	22.4	57.5	63.8
Eagle-13B [85]	74.0	77.6	54.4	75.7	-	42.6	41.6	-	21.8	60.2	62.9
VILA1.5-8B [59]	58.8	-	37.3	75.3	69.9	43.2	38.6	-	39.5	45.2	43.4
VILA1.5-13B [59]	69.9	-	42.5	74.9	66.3	44.3	37.9	-	48.1	50.2	53.3
CogVLM2-19B [37]	73.4	81.0	38.6	80.5	-	60.4	44.3	-	-	66.0	62.9
LLaVA-OneVision-7B [53]	81.4	80.0	63.2	80.8	-	57.5	48.8	24.1	53.0	65.4	69.9
InternVL2-8B [22]	83.8	83.3	58.3	81.7	81.2	54.2	49.3	29.0	50.9	67.3	64.2
MiniCPM-V2.5-8B [112]	78.4	-	54.3	77.2	74.2	52.8	45.8	-	-	61.4	63.5
MiniCPM-V2.6-8B [112]	82.1	-	60.6	-	-	60.0	49.8	27.2	55.2	65.7	65.0
Qwen2-VL-7B [105]	77.5	83.0	58.2	83.0	80.5	62.0	54.1	30.5	53.8	68.6	68.5
InternVL2.5-8B [20]	84.8	84.8	64.4	84.6	82.6	62.8	56.0	34.3	54.8	69.7	70.1
Qwen2-VL-7B-GenRecal (InternVL2.5-78B)	**93.9**	**95.3**	68.8	88.4	87.4	70.4	65.6	**49.6**	64.3	70.7	79.2
InternVL2.5-8B-GenRecal (InternVL2.5-78B)	93.0	93.6	**74.9**	**89.5**	**88.2**	**73.2**	**68.1**	48.8	**65.3**	**72.3**	**81.4**
VILA1.5-3B [59]	57.9	-	31.6	-	-	38.8	34.2	-	39.7	41.4	53.2
Phi-3.5-Vision-4B [1]	77.8	81.8	43.9	76.0	66.1	43.2	43.0	19.7	58.3	62.2	53.6
InternVL2-4B [22]	78.9	81.5	58.6	78.6	73.9	51.0	34.3	32.7	46.1	63.9	60.7
InternVL2.5-4B [22]	81.4	84.0	60.5	81.1	79.3	60.6	52.3	32.7	50.8	66.9	64.3
InternVL2.5-4B-GenRecal (InternVL2.5-78B)	**90.0**	**91.1**	**70.4**	**88.4**	**86.2**	**66.1**	**58.3**	**45.9**	**63.5**	**69.3**	**75.2**
InternVL2-2B [22]	74.1	76.2	46.3	73.2	70.9	39.5	34.3	18.2	43.8	60.0	57.3
Qwen2-VL-2B [105]	60.2	73.5	43.0	74.9	73.5	49.5	41.1	21.2	45.2	61.2	62.6
Aquila-VL-2B [20]	75.0	76.5	59.0	-	-	43.8	47.4	-	34.1	63.0	65.0
InternVL2.5-2B [20]	74.9	79.2	51.3	74.7	71.9	60.8	43.6	23.7	44.0	60.0	60.1
Qwen2-VL-2B-GenRecal (InternVL2.5-78B)	89.1	**90.9**	60.5	82.9	81.0	57.3	52.9	**37.5**	53.4	65.5	72.8
InternVL2.5-2B-GenRecal (InternVL2.5-78B)	**91.8**	90.7	**62.5**	**84.1**	**80.4**	**61.2**	**59.2**	36.6	**55.5**	**67.3**	**73.0**
LLaVA-OneVision-0.5B [53]	57.1	61.4	34.8	61.6	55.5	32.2	31.4	-	52.1	45.7	55.6
InternVL2-1B [22]	64.1	72.9	37.7	65.4	60.7	32.7	36.7	14.8	38.6	54.3	50.3
InternVL2.5-1B [20]	69.3	75.9	43.2	70.7	66.3	48.8	40.9	19.4	42.0	59.0	57.5
InternVL2.5-1B-GenRecal (InternVL2.5-78B)	**82.9**	**89.4**	**56.5**	**80.1**	**74.4**	**54.4**	**45.6**	**28.7**	**48.5**	**65.1**	**70.8**

sequently passed through *Proj-post* to restore the hidden dimensionality of the large VLM. This forward rule of Recalibrator is illustrated in Fig. 3(c).

Finally, the answer part of the resulting features $[r_{q_s}, r_{a_l}] = \mathit{Recalibrator}([z_{q_s}, z_{a_l}])$ are fed into *VLM-head* of the large VLM to compute the autoregressive loss:

$$\mathcal{L}_{ar} = \mathrm{CE}(\mathit{VLM\text{-}head}_l(r_{a_l}), gt_l), \tag{2}$$

where gt_l means answer token index from large VLM. Additionally, we employ a KL divergence loss to further enhance Recalibrator's projection capability in first training stage and distill the knowledge from the teacher in second training stage. This process enables the large VLM to interpret the hidden features of the small VLM, thus establishing a bridge for general-purpose distillation across heterogeneous token types.

3.3 Training Process

To achieve general-purpose distillation, we adopt a three-stage training process. In the first stage, only Recalibrator is trained while keeping all parameters of both the large and small VLMs frozen, as illustrated in Fig. 3(a). During this stage, we compute both the autoregressive loss and the KL divergence, described in Algorithm 1 where the purple components indicate the trainable parameters. This step primarily serves to align the feature representations between the large and small VLMs. For the first stage, we introduce regularization loss, as illustrated in Fig. 4, which is designed to prevent the feature representations of Recalibrator from drifting too far from those of the large VLM. We both use Algorithm 1 and Algorithm 2 at the same time for conducting first stage.

Table 2: (b) Comparison of GenRecal with large-scale open-source and closed-source VLMs on challenging benchmarks: MMB [64], MM-Vet [115], MM-Vet-v2 [116], MMMU [117], MMMU-Pro [118], MMStar [15], AI2D [44], ChartQA [69], SEED-2-Plus [54], MathVista [66], BLINK [32], RealWorldQA (RWQA).

VLMs	MMB	MM-Vet	MM-Vet-v2	MMMU	MMMU-Pro	MMStar	AI2D	ChartQA	SEED-2-Plus	MathVista	BLINK	RWQA
NVLM-72B [26]	-	58.9	-	59.7	-	63.7	85.2	86.0	68.4	66.6	48.0	69.9
LLaVA-OneVision-72B [53]	85.8	60.6	-	56.8	31.0	65.8	85.6	83.7	-	67.5	55.4	71.9
Molmo-72B [28]	-	61.1	-	54.1	-	63.3	83.4	87.3	-	58.6	-	73.7
Qwen2-VL-72B [105]	86.5	74.0	68.7	64.5	46.2	68.3	88.1	88.3	**72.3**	70.5	60.5	77.8
InternVL2-76B [22]	86.5	65.7	68.4	62.7	40.0	67.4	87.6	88.4	69.7	65.5	56.8	72.2
InternVL2.5-78B [53]	88.3	72.3	65.5	**70.1**	48.6	**69.5**	89.1	88.3	71.3	72.3	63.8	78.7
Claude-3.5-Sonnet [4]	82.6	70.1	**71.8**	68.3	51.5	65.1	81.2	90.8	71.7	67.7	60.1	60.1
Gemini-1.5-Pro [94]	73.9	64.0	66.9	62.2	46.9	59.1	79.1	87.2	70.8	63.9	59.1	67.5
GPT-4o (0513) [74]	83.4	69.1	71.0	69.1	**51.9**	64.7	84.6	85.7	72.0	63.8	**68.0**	75.4
InternVL2.5-8B-GenRecal (NVLM-72B)	88.8	63.9	59.3	60.3	34.7	65.1	88.5	84.3	69.3	67.5	55.6	72.5
InternVL2.5-8B-GenRecal (InternVL2-76B)	89.0	72.4	65.0	64.6	42.8	65.8	92.1	90.4	70.9	71.9	57.7	75.5
InternVL2.5-8B-GenRecal (Qwen2-VL-72B)	**89.5**	71.4	62.6	65.6	43.8	66.1	92.2	87.5	71.3	71.4	61.4	78.8
InternVL2.5-8B-GenRecal (InternVL2.5-78B)	**89.5**	**73.2**	67.2	68.1	48.8	67.8	**93.0**	**93.6**	**72.3**	**74.9**	65.3	**81.4**

In the second stage, we keep using the same loss functions of the first stage and additionally incorporate the small VLM's own autoregressive loss in Algorithm 3. As depicted in Fig. 3(b), this stage enables knowledge distillation from the large VLM to the small one by training the small VLM's *VLM-body*. In the final stage, we remove both Recalibrator and the large VLM, and fine-tune the student VLM. Specifically, we train all parameters of the student VLM except for the vision encoder through supervised fine-tuning (SFT) to further enhance its instruction-following capability.

4 Experiments

4.1 Implementation Detail

To ensure successful reproducibility, we outline three key technical aspects and details of GenRecal: (a) the structure detail of Recalibrator and (b) projection layers (c) specific details of training and evaluation.

(a) Structure Detail of Recalibrator. This is composed of two transformer decoder blocks (*Rec-body*) and two projectors (*Proj-pre* and *Proj-post*). The decoder blocks follow all configurations of small VLMs' decoder block such as causal mask, hidden dimensions, number of heads, and FFN structure. The reason why transformer decoder blocks are used for *Rec-body* is because we should handle the concatenated student and teacher features in Fig. 3, and they are sequence that transformer decoder normally treat. Even, these features should preserve token ordering, so we additionally introduce new positional embeddings (NPE) to adapt it. This design enables effective sequential modeling and representation alignment between heterogeneous VLMs. To realize it, we employ additional RoPE [90] to realign their positional embeddings, and their position IDs are re-assigned as well. Lastly, we apply additional layer-norm [6] into the output features of Recalibrator for stable adaptation.

(b) Projection Layer Design. Two projection layers (*Proj-pre* and *Proj-post*) are linear layers introduced for hidden dimension matching. Similar to the role of vision projector that matches the hidden dimensions between a CLIP-like vision encoder and an LLM, *Proj-pre* matches the teacher features to the student hidden dimension, while *Proj-post* restores the dimension back to the teacher

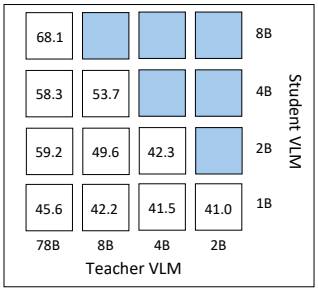

Fig. 5: Distillation performance on MMMU [117] for various pairings os teacher and student VLM. Each cell indicates the resulting score when using the corresponding teacher (rows) and student (columns) model sizes.

hidden dimension so that the large *VLM-head* can be utilized for distillation. This explanation is technically depicted in Fig. 3(c) and Fig. 4.

(c) Details of Training and Evaluation. By using DeepSpeed engine with ZeRO-3 [80], we train and evaluate GenRecal on 128 NVIDIA A100 80GB GPUs. We use AdamW optimizer [65] and apply a linearly decayed learning rate from 1e-4 to 1e-5 at each training stage. The first and second stages utilize the entire 9M dataset (see Appendix E for dataset composition and analysis), which are taken approximately 2 to 4 hours and 8 to 11 hours respectively depending on the model sizes. The last stage is taken 4 to 6 hours by using a 6M dataset which is the sample collections after removing general visual question answering [53]. For stable training, we handle large batch sizes by using gradient accumulation with 16 steps. We use 4 (first and third stage) or 2 (second stage) batches per one GPU, leading to total 8192 (128×16×4) or 4096 (128×16×2) batches. For evaluation, we remove Recalibrator and large VLMs, and we make small VLMs generate answers by using the default generation hyperparameter.

4.2 Validation and Analysis for GenRecal

Higher Size, Higher Performance. Throughout its realization of GenRecal, Tab. 1 demonstrates that GenRecal outperforms not only previous standard model size VLMs but also smaller size VLMs, highlighting that GenRecal generalizes well across different model sizes. From this table, we can say that choosing more high-performing small VLMs like InternVL2.5-8B [20] significantly impacts the overall distillation results as well. Furthermore, when we choose same large VLMs, selecting more smaller size VLMs makes the lower distillation performances in the end. It implies that employing more capable small VLMs is crucial for achieving higher distillation performances.

Next, we examine the effect of changing large VLMs to determine whether the aforementioned property holds consistently across different large VLMs. As shown in Fig. 2 and Tab. 2, we can see that selecting more powerful large VLMs leads to greater performance improvements. To further investigate it, we utilize InternVL2.5 series [20] and conduct experiments with various combinations of large and small VLM sizes, as illustrated in Fig. 5. The results also consistently

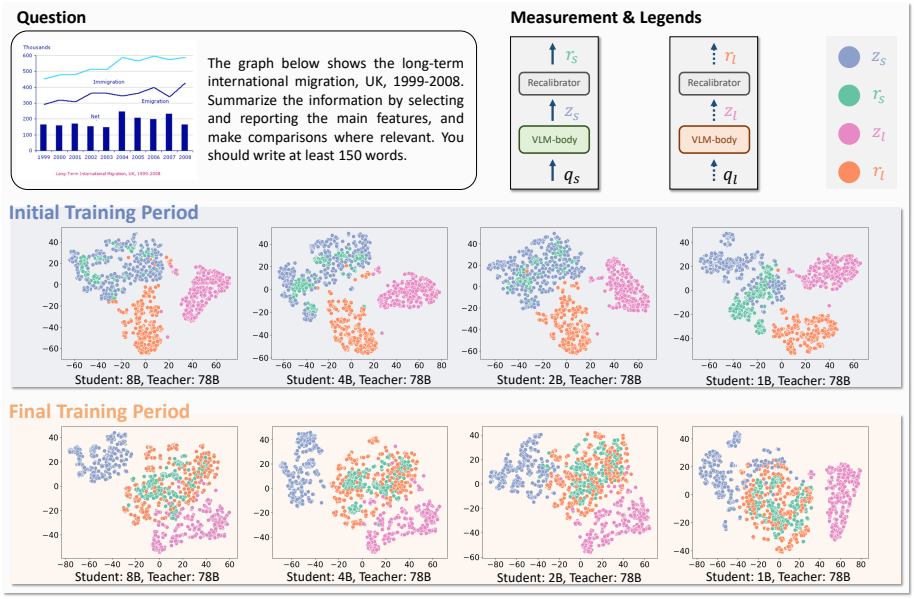

Fig. 6: An overview of our training pipeline, illustrating both the question prompt and the measurement/legend annotations (top), followed by t-SNE visualizations (bottom) of teacher and student VLM pairings at the initial and final training stages. The question prompt (upper-left) shows the format of the question, while the measurement and legend box (upper-right) shows key model components to measure. Each scatter plot in the lower panels corresponds to a different combination of teacher and student VLM sizes, capturing how the learned representations evolve from early to later training.

indicates that choosing larger size teacher and student VLMs eventually leads to higher distillation performances.

Analysis of Recalibrator. We shift our focus to Recalibrator in order to explore its role in general-purpose distillation. First, we show that loss graphs for building Recalibrator are converged stably based on various combinations of large and small VLMs (see Appendix D). Since the losses for training Recalibrator ('Recalib(q_s, a_l)' and 'Recalib(q_l, a_l)') are minimized well compared with the perplexity of 'SmallVLM(q_s, a_s)' and 'LargeVLM(q_l, a_l)', we can infer that Recalibrator successfully aligns the feature representations of large and small VLMs. It suggests that Recalibrator generalizes well in various combinations of teacher and student VLMs. Furthermore, Fig. 6 visualizes multiple feature spaces to identify whether the features of large and small VLMs after Recalibrator are really matched and whether we can consider them as shared feature representation. From this figure, the features of small VLMs before Recalibrator are initially close to the features of small VLMs after Recalibrator, but they are getting matched to the features of large VLMs after Recalibrator at the final training period. Based on this, we can interpret that Recalibrator is really helpful to make the shared feature representation for large and small VLMs.

Table 3: Comparing the final distillation performances from the teacher model: InternVL2.5-78B [20] with and without the regularization term (denoted as "Reg"). Note that, the student models are each InternVL2.5-8B, 4B, 2B, and 1B.

VLMs	Reg	MMB	MathVista	MM-Vet	MMMU
InternVL2.5-8B	-	84.6	64.4	62.8	56.0
w. GenRecal	✗	88.2	69.8	63.5	58.9
w. GenRecal	✓	**89.5**	**74.9**	**73.2**	**68.1**
InternVL2.5-4B	-	81.1	60.5	60.6	52.3
w. GenRecal	✗	82.9	61.7	61.1	53.6
w. GenRecal	✓	**88.4**	**70.4**	**66.1**	**58.3**
InternVL2.5-2B	-	74.7	51.3	60.8	43.6
w. GenRecal	✗	75.8	53.2	60.9	45.4
w. GenRecal	✓	**84.1**	**62.5**	**61.2**	**59.2**
InternVL2.5-1B	-	70.7	43.2	48.8	40.9
w. GenRecal	✗	72.6	45.9	49.8	41.1
w. GenRecal	✓	**80.1**	**56.5**	**54.4**	**45.6**

Table 4: Comparing SFT, traditional distillations, and GenRecal where we use equal training dataset (Section 4.1(b)) and choose the teacher (Qwen2-VL-72B [105]) that has the same token type of student.

VLMs	MMB	MathVista	MM-Vet	MMMU
Qwen2-VL-7B	83.0	58.2	62.0	54.1
w. SFT	84.3	60.5	64.2	56.3
w. MiniLLM	84.4	61.3	65.1	57.4
w. DistiLLM	84.8	61.5	65.3	57.9
w. LLaVA-KD	85.0	61.8	65.9	58.2
w. GenRecal	**87.8**	**69.5**	**67.8**	**64.2**
Qwen2-VL-2B	74.9	43.0	49.5	41.1
w. SFT	76.3	45.8	51.8	44.3
w. MiniLLM	77.5	46.2	52.5	45.3
w. DistiLLM	77.9	46.6	53.0	46.1
w. LLaVA-KD	78.3	46.9	53.7	46.9
w. GenRecal	**82.9**	**58.3**	**57.1**	**51.4**

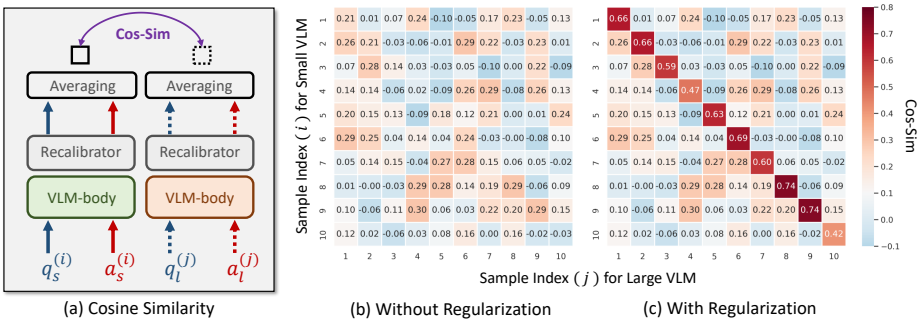

(a) Cosine Similarity (b) Without Regularization (c) With Regularization

Fig. 7: The process of (a) computing cosine similarity, (b) the result without regularization or (c) with regularization. Because the number of the embedded tokens for small and large VLMs are naturally different due to vocabulary size, token split, and token ordering, therefore we do average the output tokens and compute cosine similarity.

Importance of Regularization. We conduct an ablation study that investigates how important the regularization term is for the final distillation performances. We first remove the regularization term and analyze the differences before and after its removal. To illustrate this in detail, we simply prepare 10 different question-answer pairs and input them through *VLM-body* of both small and large VLMs. Afterwards, we propagate their output features into Recalibrator, as described in Fig. 7(a). We then compute a 10×10 cosine similarity matrix between Recalibrator's output features from the small and large VLMs. To ensure reliable cosine similarity values, we use all training dataset samples and compute the average of the cosine similarity values for all the samples.

With the regularization term included, as shown in Fig. 7(c), we observe that the diagonal values in the cosine similarity matrix are significantly higher than the off-diagonal values. This implies that the features of small and large VLMs are explicitly shared through Recalibrator, aligned with the results in Fig. 6 as well. In contrast, when the regularization term is removed, as depicted in Fig. 7(b), the diagonal values are comparable with the off-diagonal values. This indicates that Recalibrator fails to explicitly align large and small VLMs' features, preventing feature matching and sharing. As a result, this leads to a significant drop in final distillation performances, as reported in Tab. 3. Insufficient

Table 5: Importance of the autoregressive loss ($\mathcal{L}_{ar}$) for representation alignment. We compare the baseline VLMs, GenRecal trained without $\mathcal{L}_{ar}$ (✗, using only $\mathcal{L}_{kl}$), and GenRecal trained with $\mathcal{L}_{ar}$ (✓), using InternVL2.5-78B [20] as the teacher VLM.

VLMs	$\mathcal{L}_{ar}$	AI2D	ChartQA	MathVista	MMB	MMB^{CN}	MM-Vet	MMMU	MMMU-Pro	BLINK	SEED-2-Plus	RWQA	Avg
Qwen2-VL-7B [105]	-	77.5	83.0	58.2	83.0	80.5	62.0	54.1	30.5	53.8	68.6	68.5	65.4
InternVL2.5-8B [20]	-	84.8	84.8	64.4	84.6	82.6	62.8	56.0	34.3	54.8	69.7	70.1	68.1
Qwen2-VL-7B-GenRecal (InternVL2.5-78B)	✗	66.2	67.5	47.8	63.4	55.9	49.6	45.8	30.5	52.1	65.3	60.9	55.0
InternVL2.5-8B-GenRecal (InternVL2.5-78B)	✗	68.4	70.1	55.2	68.9	62.5	55.4	50.6	35.1	58.7	68.2	64.4	59.8
Qwen2-VL-7B-GenRecal (InternVL2.5-78B)	✓	93.9	95.3	68.8	88.4	87.4	70.4	65.6	49.6	64.3	70.7	79.2	75.8
InternVL2.5-8B-GenRecal (InternVL2.5-78B)	✓	93.0	93.6	74.9	89.5	88.2	73.2	68.1	48.8	65.3	72.3	81.4	77.1

alignment of large and student VLMs reduces efficient knowledge transfer during distillation. These findings highlight the crucial role of the regularization term in feature alignment and knowledge transfer for general-purpose distillation.

Autoregressive Loss for Representation Alignment. To align the student representations with the teacher's latent space, GenRecal uses two objectives: KL divergence loss ($\mathcal{L}_{kl}$) and autoregressive loss ($\mathcal{L}_{ar}$). The KL divergence loss performs standard distillation by matching the logit-level distribution of teacher and student. However, matching distributions alone does not guarantee precise alignment at the token level. The autoregressive loss provides explicit hard-target supervision, allowing it to predict the exact ground-truth token sequence. In short, $\mathcal{L}_{kl}$ transfers knowledge at the distribution level, whereas $\mathcal{L}_{ar}$ ensures exact alignment in the token space-level. As shown in Tab. 5, removing $\mathcal{L}_{ar}$ consistently degrades performance across benchmarks, confirming that autoregressive supervision is essential for effective representation alignment.

4.3 Ablation Studies: Training Computation and Configurations

In Tab. 6(a), we compare the model sizes and training FLOPs of the small VLM, large VLM, and Recalibrator to assess whether Recalibrator introduces additional computational overhead during training. The results show that Recalibrator's FLOPs are substantially lower than those of both the large and small VLMs. Note that Recalibrator is removed at inference time, thus incurring no additional computational cost during inference. We further conduct a series of ablation studies to examine various configurations affecting the distillation performance of GenRecal. As shown in Tab. 6(b), we vary the decoder depth of Recalibrator from 1 to 20 and select two depths for layer number of *Rec-body* based on a trade-off between computational efficiency and performance. Additionally, Tab. 6(c) demonstrates the importance of employing a new positional embedding (NPE) to handle newly introduced position IDs and to integrate RoPE [90] from both large and small VLMs, which have different token types.

To analyze the effect of dataset scale, we control the dataset size from 1M to 9M samples, as shown in Tab. 6(d). The performance improvements between 5M and 9M samples are marginal, suggesting that a 5M dataset is a practical choice for users with limited training resources. Furthermore, Tab. 6(e) shows that fine-tuning the large VLM on our dataset yields further gains, indicating that the small VLM trained under the same setting has the potential to match or even surpass the large VLM's performance.

Table 6: FLOPs comparison and several ablation studies on various configurations influencing the performance of GenRecal. Note that the teacher VLM in (b), (c), (d), (e), and (f) is InternVL2.5-78B [20], and the student VLM in (b) is InternVL2.5-8B [20].

(a) Model Size and FLOPs

Small VLM	Large VLM	Recalibrator Size
Qwen2-VL-7B (25.7×10^{12})	Qwen2-VL-72B (260×10^{12})	524.8M (2.27×10^{12})
InternVL2.5-8B (27.1×10^{12})	InternVL2.5-78B (269×10^{12})	503.3M (2.2×10^{12})
InternVL2.5-8B (27.1×10^{12})	Qwen2-VL-72B (260×10^{12})	503.3M (2.2×10^{12})
Qwen2-VL-7B (25.7×10^{12})	InternVL2.5-78B (269×10^{12})	524.8M (2.27×10^{12})

(b) Recalibrator Depth

Depths	MMB	MathVista	MM-Vet	MMMU	Avg
20	79.9	72.1	72.6	68.3	76.7
15	89.8	75.2	73.5	69.4	76.7
10	89.6	75.0	73.4	68.3	76.6
5	89.4	74.8	73.3	68.2	76.4
2	89.5	74.9	73.2	68.1	76.4
1	88.9	73.0	72.0	67.5	74.9

(c) Effect of NPE

VLM	NPE	MMB	MathVista	MM-Vet	MMMU	Avg
Qwen2-VL-7B-GenRecal	✗	79.2	60.0	64.0	63.9	66.8
Qwen2-VL-7B-GenRecal	✓	**88.4**	**68.8**	**70.4**	**65.6**	**73.3**
InternVL2.5-8B-GenRecal	✗	85.2	65.1	67.3	64.4	70.5
InternVL2.5-8B-GenRecal	✓	**89.5**	**74.9**	**73.2**	**68.1**	**76.4**

(d) Training Dataset Size

Dataset Size	MMB	MathVista	MM-Vet	MMMU	Avg
9M	**89.5**	**74.9**	**73.2**	**68.1**	**76.4**
7M	89.4	74.7	73.0	67.8	76.2
5M	89.3	74.5	72.8	67.6	76.0
3M	88.9	73.6	71.9	66.6	75.3
1M	86.6	68.6	67.0	60.9	70.8
0M	84.6	64.4	62.8	56.0	67.0

(e) Fine-Tuning

VLM	Finetuned	MMB	MathVista	MM-Vet	MMMU	Avg
InternVL2.5-78B [20]	✗	88.3	72.3	72.3	70.1	75.8
InternVL2.5-78B-SFT	✓	**89.4**	**75.2**	**74.2**	**71.7**	**77.6**
InternVL2.5-8B [20]	✗	84.6	64.4	62.8	56.0	67.0
InternVL2.5-8B-SFT	✓	86.5	65.2	65.0	59.9	69.2
InternVL2.5-8B-GenRecal	✓	**89.5**	**74.9**	**73.2**	**68.1**	**76.4**

(f) Cross-Tokenizer Methods

VLM	MathVista	MMB	MM-Vet	MMMU	Avg
InternVL2.5-8B	64.4	84.6	62.8	56.0	67.0
InternVL2.5-8B-ULD [10]	66.5	86.2	64.1	60.8	69.4
InternVL2.5-8B-MOT [25]	68.4	87.5	65.0	62.3	70.8
InternVL2.5-8B-GenRecal	**74.9**	**89.5**	**73.2**	**68.1**	**76.4**

(g) Different LLMs

LLMs	MMLU	GPQA	MATH	Avg
Qwen2-7B [111]	70.8	38.4	48.6	52.6
Qwen2-7B-GenRecal (Llama-3-70B)	78.4	38.9	49.1	55.5
Llama-3-70B [30]	**82.5**	**39.5**	**50.4**	**57.5**
InternLM2.5-7B [12]	72.8	38.4	60.1	57.1
InternLM2.5-7B-GenRecal (Qwen2.5-72B)	83.7	43.6	61.8	63.0
Qwen2.5-72B [111]	**86.1**	**45.9**	**62.1**	**64.7**

(h) Different VLM Family

VLM	MM-Vet	MathVista	MMMU	Avg
Ovis1.6-Gemma-9B [67]	65.0	67.3	55.0	62.4
Ovis1.6-Gemma-9B-GenRecal (InternVL2.5-78B)	**74.0**	**75.3**	67.7	**72.3**
InternVL2.5-78B	72.3	72.3	**70.1**	71.6
InternVL2.5-8B [20]	62.8	64.4	56.0	61.1
InternVL2.5-8B-GenRecal (Ovis1.6-Gemma-27B)	**68.5**	**69.9**	61.2	**66.5**
Ovis1.6-Gemma-27B [67]	67.2	69.7	**61.7**	66.2

(i) Recent VLMs

VLM	MMB	MathVista	MM-Vet	MMMU	Avg
Qwen3-VL-4B [7]	86.8	77.2	74.5	60.6	77.0
Qwen3-VL-4B (Qwen3-VL-32B)	**89.9**	80.1	**77.6**	**72.7**	**80.1**
Qwen3-VL-4B (InternVL3.5-38B)	89.7	**80.3**	77.4	72.2	80.0
InternVL3.5-8B [107]	86.5	78.4	83.1	73.4	80.4
InternVL3.5-8B (Qwen3-VL-32B)	**89.6**	**81.5**	86.0	76.3	**83.4**
InternVL3.5-8B (InternVL3.5-38B)	89.4	81.1	**86.2**	**76.5**	**83.4**
Qwen3-VL-32B [7]	90.6	83.8	79.4	76.0	82.5
InternVL3.5-38B [107]	90.3	81.9	82.2	76.9	82.8

We also compare GenRecal with recent cross-tokenizer distillation methods in Tab. 6(f). These baselines perform feature-level distillation via cross-token matching in the logit space by using classical method of Wasserstein distance [10] or optimal transport [25], whereas GenRecal explicitly introduces Recalibrator to align hidden features for semantic correspondence. As observed, GenRecal achieves a substantial improvement over prior approaches. It will be discussed in the next section. Lastly, Tab. 6(g)–(i) demonstrate GenRecal's strong compatibility across different LLMs, VLM Family, and recently released VLMs. In all cases, GenRecal consistently delivers superior performance, validating its general applicability to diverse model architectures.

4.4 Discussion

Representation Mismatch Beyond Tokenizer Mismatch. Basically, InternVL2.5 family [20] does not share the same tokenizer across model scales: InternVL2.5-8B uses the InternLM2.5 tokenizer [12], whereas InternVL2.5-78B uses Qwen2.5 tokenizer [111], as shown in Fig. 1. On the other hands, Qwen2-VL-72B and Qwen2-VL-7B has same Qwen2 tokenizer [111]. Importantly, even when the tokenizer is the same, a large parameter gap between the teacher and the student introduces a representation mismatch. Conventional distillation transfers knowledge from the large VLM head to the small VLM head, which can become a bottleneck because the student head has a much lower hidden dimensionality. In contrast, GenRecal performs distillation exclusively through the large VLM head, as illustrated in Fig. 3. This has two advantages: (1) the large VLM head provides a higher-capacity and more expressive representation space, and (2) Recalibrator explicitly aligns the student's hidden representations with the teacher's feature space, serving as a representation-level warm-up before distillation. This explains why GenRecal improves performance even under the same tokenizer setting, as demonstrated in Tab. 4. We further compare GenRecal with traditional distillation methods under identical token types for both teacher and student VLMs. Specifically, we use Qwen2-VL series [105] as the teacher (72B) and student (7B or 2B) VLMs. Interestingly, even when limited to the same token types, Tab. 4 shows that GenRecal outperforms both SFT and

Table 7: Comparison of computational cost (FLOPs and Training Time) and performance across cross-tokenizer distillation methods. We average performance across four benchmarks: MMB [64], MathVista [66], MM-Vet [115], and MMMU [117].

Method	Extra	FLOPs	Training Stages	Training Time	Avg. Perform.
GenRecal	Recalibrator	298.3×10^{12}	3	3.1+10.4+5.3=**18.8** hours	**76.4**
ULD [10]	Vocab Matching	296.1×10^{12}	1	11.1×2(Epochs)=22.2 hours	69.4
MOT [25]	Optimal Transport	296.1×10^{12}	1	12.5×2(Epochs)=25.0 hours	70.8

traditional distillation by a substantial margin. Note that MiniLLM [34] employs reverse KL divergence, DistiLLM [46] uses a skewed variant, and LLaVA-KD [11] applies normal KL divergence within a three-stage framework. These results suggest even when the large and small VLMs share identical token types, explicit feature alignment remains crucial to reduce representational disparity.

Cross-Token Matching. We can divide cross-token matching into two cases: (a) word embedding (vocabulary) matching and (b) semantic feature matching. Fundamentally, case (a) is infeasible because the backbone decoder still cannot understand different word embeddings without retraining the entire model from scratch. For case (b), ULD [10] and MOT [25] have recently been proposed as solutions for cross-token matching, which we compared in Tab. 6(f). They aim to match probability mass geometry across vocabularies via token-wise Wasserstein distance or optimal transport in the logit space, but these approaches suffer from potential information loss since they cannot properly handle token-split indices, leading to mismatched output lengths during distillation. To overcome them, they just rely on zero-padding or truncation to enforce equal token lengths. In contrast, GenRecal does not perform token-level matching at the logit space. Instead, GenRecal aligns student and teacher representations before the language head through a learnable Recalibrator, enabling the teacher *VLM-head* to directly interpret student features. As a result, GenRecal does not require token-wise correspondence, probability sorting, padding, or transport cost design. Besides, we analyze the computation complexity and its corresponding average performance. As shown in Tab. 6(a), Recalibrator introduces only a small fraction of FLOPs compared to both the teacher and student VLMs. Consequently, the overall FLOPs of GenRecal are comparable to recent cross-tokenizer distillation frameworks in Tab. 6(f), but they require at least 2 epochs to reach the performance that we achieved. Based on Tab. 7, we found that even if GenRecal requires multi training stages and new components, the additional computational overhead is comparable but achieves the highest performance. Note that we experimented them under same settings where same training dataset is used and we regard InternVL2.5-8B [20] as student and InternVL2.5-78B [20] as teacher.

5 Conclusion

We present a new, efficient family of vision-language models (VLMs) called **Gen**eration after **Recal**ibration (GenRecal). At its core, Recalibrator enables token types-compatible general-purpose distillation. For future improvements, we will expand intermediate layer's Recalibrator to embed fine-grained and se-

quential knowledge, or multiple VLMs-source distillation. We envision GenRecal as a pivotal framework in the field of distillation, providing a versatile scheme.

References

1. Abdin, M., Jacobs, S.A., Awan, A.A., Aneja, J., Awadallah, A., Awadalla, H., Bach, N., Bahree, A., Bakhtiari, A., Behl, H., et al.: Phi-3 technical report: A highly capable language model locally on your phone. arXiv preprint arXiv:2404.14219 (2024)
2. Agarwal, R., Vieillard, N., Zhou, Y., Stanczyk, P., Garea, S.R., Geist, M., Bachem, O.: On-policy distillation of language models: Learning from self-generated mistakes. In: The Twelfth International Conference on Learning Representations (2024)
3. Alayrac, J.B., Donahue, J., Luc, P., Miech, A., Barr, I., Hasson, Y., Lenc, K., Mensch, A., Millican, K., Reynolds, M., et al.: Flamingo: a visual language model for few-shot learning. Advances in Neural Information Processing Systems **35**, 23716–23736 (2022)
4. Anthropic: The claude 3 model family: Opus, sonnet, haiku. `https://www.anthropic.com` (2024), `https://www-cdn.anthropic.com/de8ba9b01c9ab7cbabf5c33b80b7bbc618857627/Model_Card_Claude_3.pdf`
5. Austin, J., Odena, A., Nye, M., Bosma, M., Michalewski, H., Dohan, D., Jiang, E., Cai, C., Terry, M., Le, Q., et al.: Program synthesis with large language models. arXiv preprint arXiv:2108.07732 (2021)
6. Ba, J.L., Kiros, J.R., Hinton, G.E.: Layer normalization (2016), `https://arxiv.org/abs/1607.06450`
7. Bai, S., Cai, Y., Chen, R., Chen, K., Chen, X., Cheng, Z., Deng, L., Ding, W., Gao, C., Ge, C., et al.: Qwen3-vl technical report. arXiv preprint arXiv:2511.21631 (2025)
8. Ben-Baruch, E., Karklinsky, M., Biton, Y., Ben-Cohen, A., Lawen, H., Zamir, N.: It's all in the head: Representation knowledge distillation through classifier sharing. arXiv preprint arXiv:2201.06945 (2022)
9. Boizard, N., Haddad, K.E., Hudelot, C., Colombo, P.: Towards cross-tokenizer distillation: the universal logit distillation loss for llms. arXiv preprint arXiv:2402.12030 (2024)
10. Boizard, N., Haddad, K.E., HUDELOT, C., Colombo, P.: Towards cross-tokenizer distillation: the universal logit distillation loss for LLMs. Transactions on Machine Learning Research (2025), `https://openreview.net/forum?id=bwRxXiGO9A`
11. Cai, Y., Zhang, J., He, H., He, X., Tong, A., Gan, Z., Wang, C., Bai, X.: Llava-kd: A framework of distilling multimodal large language models. arXiv preprint arXiv:2410.16236 (2024)
12. Cai, Z., Cao, M., Chen, H., Chen, K., Chen, K., Chen, X., Chen, X., Chen, Z., Chen, Z., Chu, P., et al.: Internlm2 technical report. arXiv preprint arXiv:2403.17297 (2024)
13. Cao, J., Zhang, Y., Huang, T., Lu, M., Zhang, Q., An, R., Ma, N., Zhang, S.: Move-kd: Knowledge distillation for vlms with mixture of visual encoders. arXiv preprint arXiv:2501.01709 (2025)
14. Chen, J., Zhu, D., Shen, X., Li, X., Liu, Z., Zhang, P., Krishnamoorthi, R., Chandra, V., Xiong, Y., Elhoseiny, M.: Minigpt-v2: large language model as a unified interface for vision-language multi-task learning. arXiv preprint arXiv:2310.09478 (2023)

15. Chen, L., Li, J., Dong, X., Zhang, P., Zang, Y., Chen, Z., Duan, H., Wang, J., Qiao, Y., Lin, D., et al.: Are we on the right way for evaluating large vision-language models? arXiv preprint arXiv:2403.20330 (2024)
16. Chen, L., Li, J., Dong, X., Zhang, P., He, C., Wang, J., Zhao, F., Lin, D.: Sharegpt4v: Improving large multi-modal models with better captions. arXiv preprint arXiv:2311.12793 (2023)
17. Chen, P., Liu, S., Zhao, H., Jia, J.: Distilling knowledge via knowledge review. In: Proceedings of the IEEE/CVF conference on computer vision and pattern recognition. pp. 5008–5017 (2021)
18. Chen, Q., Qin, L., Zhang, J., Chen, Z., Xu, X., Che, W.: M^3cot: A novel benchmark for multi-domain multi-step multi-modal chain-of-thought. In: Proc. of ACL (2024)
19. Chen, Y., Hu, H., Luan, Y., Sun, H., Changpinyo, S., Ritter, A., Chang, M.W.: Can pre-trained vision and language models answer visual information-seeking questions? arXiv preprint arXiv:2302.11713 (2023)
20. Chen, Z., Wang, W., Cao, Y., Liu, Y., Gao, Z., Cui, E., Zhu, J., Ye, S., Tian, H., Liu, Z., et al.: Expanding performance boundaries of open-source multimodal models with model, data, and test-time scaling. arXiv preprint arXiv:2412.05271 (2024)
21. Chen, Z., Wang, W., Tian, H., Ye, S., Gao, Z., Cui, E., Tong, W., Hu, K., Luo, J., Ma, Z., et al.: How far are we to gpt-4v? closing the gap to commercial multimodal models with open-source suites. arXiv preprint arXiv:2404.16821 (2024)
22. Chen, Z., Wu, J., Wang, W., Su, W., Chen, G., Xing, S., Muyan, Z., Zhang, Q., Zhu, X., Lu, L., et al.: Internvl: Scaling up vision foundation models and aligning for generic visual-linguistic tasks. arXiv preprint arXiv:2312.14238 (2023)
23. Chung, H.W., Hou, L., Longpre, S., Zoph, B., Tay, Y., Fedus, W., Li, Y., Wang, X., Dehghani, M., Brahma, S., et al.: Scaling instruction-finetuned language models. arXiv preprint arXiv:2210.11416 (2022)
24. Conneau, A., Lample, G., Ranzato, M., Denoyer, L., Jégou, H.: Word translation without parallel data. arXiv preprint arXiv:1710.04087 (2017)
25. Cui, X., Zhu, M., Qin, Y., Xie, L., Zhou, W., Li, H.: Multi-level optimal transport for universal cross-tokenizer knowledge distillation on language models. In: Proceedings of the AAAI Conference on Artificial Intelligence. vol. 39, pp. 23724–23732 (2025)
26. Dai, W., Lee, N., Wang, B., Yang, Z., Liu, Z., Barker, J., Rintamaki, T., Shoeybi, M., Catanzaro, B., Ping, W.: Nvlm: Open frontier-class multimodal llms. arXiv preprint (2024)
27. Dai, W., Li, J., Li, D., Tiong, A., Zhao, J., Wang, W., Li, B., Fung, P., Hoi, S.: InstructBLIP: Towards general-purpose vision-language models with instruction tuning. In: Thirty-seventh Conference on Neural Information Processing Systems (2023)
28. Deitke, M., Clark, C., Lee, S., Tripathi, R., Yang, Y., Park, J.S., Salehi, M., Muennighoff, N., Lo, K., Soldaini, L., et al.: Molmo and pixmo: Open weights and open data for state-of-the-art multimodal models. arXiv preprint arXiv:2409.17146 (2024)
29. Dong, X., Zhang, P., Zang, Y., Cao, Y., Wang, B., Ouyang, L., Zhang, S., Duan, H., Zhang, W., Li, Y., et al.: Internlm-xcomposer2-4khd: A pioneering large vision-language model handling resolutions from 336 pixels to 4k hd. arXiv preprint arXiv:2404.06512 (2024)

30. Dubey, A., Jauhri, A., Pandey, A., Kadian, A., Al-Dahle, A., Letman, A., Mathur, A., Schelten, A., Yang, A., Fan, A., et al.: The llama 3 herd of models. arXiv preprint arXiv:2407.21783 (2024)
31. Feng, Q., Li, W., Lin, T., Chen, X.: Align-kd: Distilling cross-modal alignment knowledge for mobile vision-language model. arXiv preprint arXiv:2412.01282 (2024)
32. Fu, X., Hu, Y., Li, B., Feng, Y., Wang, H., Lin, X., Roth, D., Smith, N.A., Ma, W.C., Krishna, R.: Blink: Multimodal large language models can see but not perceive. arXiv preprint arXiv:2404.12390 (2024)
33. Gu, S., Zhang, J., Zhou, S., Yu, K., Xing, Z., Wang, L., Cao, Z., Jia, J., Zhang, Z., Wang, Y., et al.: Infinity-mm: Scaling multimodal performance with large-scale and high-quality instruction data. arXiv preprint arXiv:2410.18558 (2024)
34. Gu, Y., Dong, L., Wei, F., Huang, M.: Minillm: Knowledge distillation of large language models. In: The Twelfth International Conference on Learning Representations (2024)
35. Heo, B., Kim, J., Yun, S., Park, H., Kwak, N., Choi, J.Y.: A comprehensive overhaul of feature distillation. In: Proceedings of the IEEE/CVF international conference on computer vision. pp. 1921–1930 (2019)
36. Hinton, G., Vinyals, O., Dean, J.: Distilling the knowledge in a neural network. arXiv preprint arXiv:1503.02531 (2015)
37. Hong, W., Wang, W., Ding, M., Yu, W., Lv, Q., Wang, Y., Cheng, Y., Huang, S., Ji, J., Xue, Z., et al.: Cogvlm2: Visual language models for image and video understanding. arXiv preprint arXiv:2408.16500 (2024)
38. Hosu, V., Lin, H., Sziranyi, T., Saupe, D.: Koniq-10k: An ecologically valid database for deep learning of blind image quality assessment. IEEE Transactions on Image Processing **29**, 4041–4056 (2020)
39. Hsieh, C.Y., Li, C.L., Yeh, C.K., Nakhost, H., Fujii, Y., Ratner, A., Krishna, R., Lee, C.Y., Pfister, T.: Distilling step-by-step! outperforming larger language models with less training data and smaller model sizes. arXiv preprint arXiv:2305.02301 (2023)
40. Hu, A., Xu, H., Ye, J., Yan, M., Zhang, L., Zhang, B., Li, C., Zhang, J., Jin, Q., Huang, F., et al.: mplug-docowl 1.5: Unified structure learning for ocr-free document understanding. arXiv preprint arXiv:2403.12895 (2024)
41. Hu, E.J., Shen, Y., Wallis, P., Allen-Zhu, Z., Li, Y., Wang, S., Wang, L., Chen, W.: Lora: Low-rank adaptation of large language models. arXiv preprint arXiv:2106.09685 (2021)
42. Huang, Z., Chen, K., He, J., Bai, X., Karatzas, D., Lu, S., Jawahar, C.: Icdar2019 competition on scanned receipt ocr and information extraction. In: 2019 International Conference on Document Analysis and Recognition (ICDAR). pp. 1516–1520. IEEE (2019)
43. Kaplan, J., McCandlish, S., Henighan, T., Brown, T.B., Chess, B., Child, R., Gray, S., Radford, A., Wu, J., Amodei, D.: Scaling laws for neural language models. arXiv preprint arXiv:2001.08361 (2020)
44. Kembhavi, A., Salvato, M., Kolve, E., Seo, M., Hajishirzi, H., Farhadi, A.: A diagram is worth a dozen images. In: Computer Vision–ECCV 2016: 14th European Conference, Amsterdam, The Netherlands, October 11–14, 2016, Proceedings, Part IV 14. pp. 235–251. Springer (2016)
45. Kirillov, A., Mintun, E., Ravi, N., Mao, H., Rolland, C., Gustafson, L., Xiao, T., Whitehead, S., Berg, A.C., Lo, W.Y., et al.: Segment anything. In: Proceedings of the IEEE/CVF International Conference on Computer Vision. pp. 4015–4026 (2023)

46. Ko, J., Kim, S., Chen, T., Yun, S.Y.: Distillm: Towards streamlined distillation for large language models. arXiv preprint arXiv:2402.03898 (2024)
47. Lee, B.K., Chung, S., Kim, C.W., Park, B., Ro, Y.M.: Phantom of latent for large language and vision models. arXiv preprint arXiv:2409.14713 (2024)
48. Lee, B.K., Chung, S., Kim, C.W., Park, B., Ro, Y.M.: Trol: Traversal of layers for large language and vision models. arXiv preprint arXiv:2406.12246 (2024)
49. Lee, B.K., Kim, C.W., Park, B., Ro, Y.M.: Meteor: Mamba-based traversal of rationale for large language and vision models. arXiv preprint arXiv:2405.15574 (2024)
50. Lee, B.K., Park, B., Kim, C.W., Ro, Y.M.: Collavo: Crayon large language and vision model. arXiv preprint arXiv:2402.11248 (2024)
51. Lee, B.K., Park, B., Kim, C.W., Ro, Y.M.: Moai: Mixture of all intelligence for large language and vision models. arXiv preprint arXiv:2403.07508 (2024)
52. Lee, Y.S., Sultan, M., El-Kurdi, Y., Naseem, T., Munawar, A., Florian, R., Roukos, S., Astudillo, R.F.: Ensemble-instruct: Instruction tuning data generation with a heterogeneous mixture of lms. In: Findings of the Association for Computational Linguistics: EMNLP 2023. pp. 12561–12571 (2023)
53. Li, B., Zhang, Y., Guo, D., Zhang, R., Li, F., Zhang, H., Zhang, K., Li, Y., Liu, Z., Li, C.: Llava-onevision: Easy visual task transfer. arXiv preprint arXiv:2408.03326 (2024)
54. Li, B., Ge, Y., Chen, Y., Ge, Y., Zhang, R., Shan, Y.: Seed-bench-2-plus: Benchmarking multimodal large language models with text-rich visual comprehension. arXiv preprint arXiv:2404.16790 (2024)
55. Li, J., Li, D., Savarese, S., Hoi, S.: Blip-2: Bootstrapping language-image pre-training with frozen image encoders and large language models. arXiv preprint arXiv:2301.12597 (2023)
56. Li, J., Li, D., Xiong, C., Hoi, S.: BLIP: Bootstrapping language-image pre-training for unified vision-language understanding and generation. In: Chaudhuri, K., Jegelka, S., Song, L., Szepesvari, C., Niu, G., Sabato, S. (eds.) Proceedings of the 39th International Conference on Machine Learning. Proceedings of Machine Learning Research, vol. 162, pp. 12888–12900. PMLR (17–23 Jul 2022)
57. Li, X., Zhang, F., Diao, H., Wang, Y., Wang, X., Duan, L.Y.: Densefusion-1m: Merging vision experts for comprehensive multimodal perception. arXiv preprint arXiv:2407.08303 (2024)
58. Li, Y., Zhang, Y., Wang, C., Zhong, Z., Chen, Y., Chu, R., Liu, S., Jia, J.: Mini-gemini: Mining the potential of multi-modality vision language models. arXiv preprint arXiv:2403.18814 (2024)
59. Lin, J., Yin, H., Ping, W., Lu, Y., Molchanov, P., Tao, A., Mao, H., Kautz, J., Shoeybi, M., Han, S.: Vila: On pre-training for visual language models. arXiv preprint arXiv:2312.07533 (2023)
60. Liu, F., Wang, X., Yao, W., Chen, J., Song, K., Cho, S., Yacoob, Y., Yu, D.: Mmc: Advancing multimodal chart understanding with large-scale instruction tuning. arXiv preprint arXiv:2311.10774 (2023)
61. Liu, H., Li, C., Li, Y., Lee, Y.J.: Improved baselines with visual instruction tuning. arXiv preprint arXiv:2310.03744 (2023)
62. Liu, H., Li, C., Li, Y., Li, B., Zhang, Y., Shen, S., Lee, Y.J.: Llava-next: Improved reasoning, ocr, and world knowledge (January 2024), `https://llava-vl.github.io/blog/2024-01-30-llava-next/`
63. Liu, H., Li, C., Wu, Q., Lee, Y.J.: Visual instruction tuning. In: Thirty-seventh Conference on Neural Information Processing Systems (2023)

64. Liu, Y., Duan, H., Zhang, Y., Li, B., Zhang, S., Zhao, W., Yuan, Y., Wang, J., He, C., Liu, Z., et al.: Mmbench: Is your multi-modal model an all-around player? arXiv preprint arXiv:2307.06281 (2023)
65. Loshchilov, I., Hutter, F.: Decoupled weight decay regularization. In: International Conference on Learning Representations (2019), https://openreview.net/forum?id=Bkg6RiCqY7
66. Lu, P., Bansal, H., Xia, T., Liu, J., Li, C., Hajishirzi, H., Cheng, H., Chang, K.W., Galley, M., Gao, J.: Mathvista: Evaluating mathematical reasoning of foundation models in visual contexts. arXiv preprint arXiv:2310.02255 (2023)
67. Lu, S., Li, Y., Chen, Q.G., Xu, Z., Luo, W., Zhang, K., Ye, H.J.: Ovis: Structural embedding alignment for multimodal large language model. arXiv:2405.20797 (2024)
68. Lu, Y., Jiang, D., Chen, W., Wang, W.Y., Choi, Y., Lin, B.Y.: Wildvision: Evaluating vision-language models in the wild with human preferences. arXiv preprint arXiv:2406.11069 (2024)
69. Masry, A., Long, D.X., Tan, J.Q., Joty, S., Hoque, E.: Chartqa: A benchmark for question answering about charts with visual and logical reasoning. arXiv preprint arXiv:2203.10244 (2022)
70. McKinzie, B., Gan, Z., Fauconnier, J.P., Dodge, S., Zhang, B., Dufter, P., Shah, D., Du, X., Peng, F., Weers, F., et al.: Mm1: Methods, analysis & insights from multimodal llm pre-training. arXiv preprint arXiv:2403.09611 (2024)
71. Mikolov, T., Chen, K., Corrado, G., Dean, J.: Efficient estimation of word representations in vector space. arXiv preprint arXiv:1301.3781 (2013)
72. Mikolov, T., Le, Q.V., Sutskever, I.: Exploiting similarities among languages for machine translation. arXiv preprint arXiv:1309.4168 (2013)
73. Muralidharan, S., Sreenivas, S.T., Joshi, R., Chochowski, M., Patwary, M., Shoeybi, M., Catanzaro, B., Kautz, J., Molchanov, P.: Compact language models via pruning and knowledge distillation. arXiv preprint arXiv:2407.14679 (2024)
74. OpenAI: Gpt-4v(ision) system card (2023), https://openai.com/research/gpt-4v-system-card, Last accessed on 2024-02-13
75. Oquab, M., Darcet, T., Moutakanni, T., Vo, H., Szafraniec, M., Khalidov, V., Fernandez, P., Haziza, D., Massa, F., El-Nouby, A., et al.: Dinov2: Learning robust visual features without supervision. arXiv preprint arXiv:2304.07193 (2023)
76. Park, W., Kim, D., Lu, Y., Cho, M.: Relational knowledge distillation. In: Proceedings of the IEEE/CVF conference on computer vision and pattern recognition. pp. 3967–3976 (2019)
77. Passalis, N., Tzelepi, M., Tefas, A.: Probabilistic knowledge transfer for lightweight deep representation learning. IEEE Transactions on Neural Networks and learning systems **32**(5), 2030–2039 (2020)
78. Radford, A., Kim, J.W., Hallacy, C., Ramesh, A., Goh, G., Agarwal, S., Sastry, G., Askell, A., Mishkin, P., Clark, J., Krueger, G., Sutskever, I.: Learning transferable visual models from natural language supervision. In: Meila, M., Zhang, T. (eds.) Proceedings of the 38th International Conference on Machine Learning. Proceedings of Machine Learning Research, vol. 139, pp. 8748–8763. PMLR (18–24 Jul 2021)
79. Raffel, C., Shazeer, N., Roberts, A., Lee, K., Narang, S., Matena, M., Zhou, Y., Li, W., Liu, P.J.: Exploring the limits of transfer learning with a unified text-to-text transformer. arXiv e-prints (2019)
80. Rajbhandari, S., Rasley, J., Ruwase, O., He, Y.: Zero: Memory optimizations toward training trillion parameter models. In: SC20: International Conference for

High Performance Computing, Networking, Storage and Analysis. pp. 1–16. IEEE (2020)
81. Riquelme, C., Puigcerver, J., Mustafa, B., Neumann, M., Jenatton, R., Susano Pinto, A., Keysers, D., Houlsby, N.: Scaling vision with sparse mixture of experts. Advances in Neural Information Processing Systems **34**, 8583–8595 (2021)
82. Romero, A., Ballas, N., Kahou, S.E., Chassang, A., Gatta, C., Bengio, Y.: Fitnets: Hints for thin deep nets. arXiv preprint arXiv:1412.6550 (2014)
83. Sanh, V., Debut, L., Chaumond, J., Wolf, T.: Distilbert, a distilled version of bert: smaller, faster, cheaper and lighter. arXiv preprint arXiv:1910.01108 (2019)
84. Shazeer, N., Mirhoseini, A., Maziarz, K., Davis, A., Le, Q., Hinton, G., Dean, J.: Outrageously large neural networks: The sparsely-gated mixture-of-experts layer. In: International Conference on Learning Representations (2017), https://openreview.net/forum?id=B1ckMDqlg
85. Shi, M., Liu, F., Wang, S., Liao, S., Radhakrishnan, S., Huang, D.A., Yin, H., Sapra, K., Yacoob, Y., Shi, H., et al.: Eagle: Exploring the design space for multimodal llms with mixture of encoders. arXiv preprint arXiv:2408.15998 (2024)
86. Shu, F., Liao, Y., Zhuo, L., Xu, C., Zhang, G., Shi, H., Chen, L., Zhong, T., He, W., Fu, S., et al.: Llava-mod: Making llava tiny via moe knowledge distillation. arXiv preprint arXiv:2408.15881 (2024)
87. Smith, S.L., Turban, D.H., Hamblin, S., Hammerla, N.Y.: Offline bilingual word vectors, orthogonal transformations and the inverted softmax. arXiv preprint arXiv:1702.03859 (2017)
88. Soldaini, L., Kinney, R., Bhagia, A., Schwenk, D., Atkinson, D., Authur, R., Bogin, B., Chandu, K., Dumas, J., Elazar, Y., Hofmann, V., Jha, A., Kumar, S., Lucy, L., Lyu, X., Lambert, N., Magnusson, I., Morrison, J., Muennighoff, N., Naik, A., Nam, C., Peters, M., Ravichander, A., Richardson, K., Shen, Z., Strubell, E., Subramani, N., Tafjord, O., Walsh, E., Zettlemoyer, L., Smith, N., Hajishirzi, H., Beltagy, I., Groeneveld, D., Dodge, J., Lo, K.: Dolma: an open corpus of three trillion tokens for language model pretraining research. In: Ku, L.W., Martins, A., Srikumar, V. (eds.) Proceedings of the 62nd Annual Meeting of the Association for Computational Linguistics (Volume 1: Long Papers). pp. 15725–15788. Association for Computational Linguistics, Bangkok, Thailand (Aug 2024). https://doi.org/10.18653/v1/2024.acl-long.840, https://aclanthology.org/2024.acl-long.840/
89. Son, W., Na, J., Choi, J., Hwang, W.: Densely guided knowledge distillation using multiple teacher assistants. In: Proceedings of the IEEE/CVF International Conference on Computer Vision. pp. 9395–9404 (2021)
90. Su, J., Ahmed, M., Lu, Y., Pan, S., Bo, W., Liu, Y.: Roformer: Enhanced transformer with rotary position embedding. Neurocomputing **568**, 127063 (2024)
91. Sujet AI, Allaa Boutaleb, H.R.: Sujet-finance-qa-vision-100k: A large-scale dataset for financial document vqa (2024), https://huggingface.co/datasets/sujet-ai/Sujet-Finance-QA-Vision-100k
92. Sun, S., Cheng, Y., Gan, Z., Liu, J.: Patient knowledge distillation for bert model compression. arXiv preprint arXiv:1908.09355 (2019)
93. Tan, H., Bansal, M.: Lxmert: Learning cross-modality encoder representations from transformers. arXiv preprint arXiv:1908.07490 (2019)
94. Team, G., Anil, R., Borgeaud, S., Wu, Y., Alayrac, J.B., Yu, J., Soricut, R., Schalkwyk, J., Dai, A.M., Hauth, A., et al.: Gemini: a family of highly capable multimodal models. arXiv preprint arXiv:2312.11805 (2023)

95. Tian, Y., Han, Y., Chen, X., Wang, W., Chawla, N.V.: Beyond answers: Transferring reasoning capabilities to smaller llms using multi-teacher knowledge distillation. arXiv preprint arXiv:2402.04616 (2024)
96. Tian, Y., Krishnan, D., Isola, P.: Contrastive representation distillation. arXiv preprint arXiv:1910.10699 (2019)
97. Timiryasov, I., Tastet, J.L.: Baby llama: knowledge distillation from an ensemble of teachers trained on a small dataset with no performance penalty. arXiv preprint arXiv:2308.02019 (2023)
98. Tong, S., Brown, E., Wu, P., Woo, S., Middepogu, M., Akula, S.C., Yang, J., Yang, S., Iyer, A., Pan, X., et al.: Cambrian-1: A fully open, vision-centric exploration of multimodal llms. arXiv preprint arXiv:2406.16860 (2024)
99. Tung, F., Mori, G.: Similarity-preserving knowledge distillation. In: Proceedings of the IEEE/CVF international conference on computer vision. pp. 1365–1374 (2019)
100. Turc, I., Chang, M.W., Lee, K., Toutanova, K.: Well-read students learn better: On the importance of pre-training compact models. arXiv preprint arXiv:1908.08962 (2019)
101. Van Horn, G., Mac Aodha, O., Song, Y., Cui, Y., Sun, C., Shepard, A., Adam, H., Perona, P., Belongie, S.: The inaturalist species classification and detection dataset. In: Proceedings of the IEEE conference on computer vision and pattern recognition. pp. 8769–8778 (2018)
102. Wan, F., Zhong, L., Yang, Z., Chen, R., Quan, X.: Fusechat: Knowledge fusion of chat models. arXiv preprint arXiv:2408.07990 (2024)
103. Wang, G.H., Ge, Y., Wu, J.: Distilling knowledge by mimicking features. IEEE Transactions on Pattern Analysis and Machine Intelligence **44**(11), 8183–8195 (2021)
104. Wang, J., Chen, Y., Zheng, Z., Li, X., Cheng, M.M., Hou, Q.: Crosskd: Cross-head knowledge distillation for object detection. In: Proceedings of the IEEE/CVF conference on computer vision and pattern recognition. pp. 16520–16530 (2024)
105. Wang, P., Bai, S., Tan, S., Wang, S., Fan, Z., Bai, J., Chen, K., Liu, X., Wang, J., Ge, W., Fan, Y., Dang, K., Du, M., Ren, X., Men, R., Liu, D., Zhou, C., Zhou, J., Lin, J.: Qwen2-vl: Enhancing vision-language model's perception of the world at any resolution (2024), https://arxiv.org/abs/2409.12191
106. Wang, W., Chen, Z., Wang, W., Cao, Y., Liu, Y., Gao, Z., Zhu, J., Zhu, X., Lu, L., Qiao, Y., et al.: Enhancing the reasoning ability of multimodal large language models via mixed preference optimization. arXiv preprint arXiv:2411.10442 (2024)
107. Wang, W., Gao, Z., Gu, L., Pu, H., Cui, L., Wei, X., Liu, Z., Jing, L., Ye, S., Shao, J., et al.: Internvl3. 5: Advancing open-source multimodal models in versatility, reasoning, and efficiency. arXiv preprint arXiv:2508.18265 (2025)
108. Woo, S., Debnath, S., Hu, R., Chen, X., Liu, Z., Kweon, I.S., Xie, S.: Convnext v2: Co-designing and scaling convnets with masked autoencoders. In: Proceedings of the IEEE/CVF Conference on Computer Vision and Pattern Recognition. pp. 16133–16142 (2023)
109. Wu, T., Tao, C., Wang, J., Yang, R., Zhao, Z., Wong, N.: Rethinking kullback-leibler divergence in knowledge distillation for large language models. arXiv preprint arXiv:2404.02657 (2024)
110. Xu, K., Rui, L., Li, Y., Gu, L.: Feature normalized knowledge distillation for image classification. In: European conference on computer vision. pp. 664–680. Springer (2020)
111. Yang, A., Yang, B., Hui, B., Zheng, B., Yu, B., Zhou, C., Li, C., Li, C., Liu, D., Huang, F., et al.: Qwen2 technical report. arXiv preprint arXiv:2407.10671 (2024)

112. Yao, Y., Yu, T., Zhang, A., Wang, C., Cui, J., Zhu, H., Cai, T., Li, H., Zhao, W., He, Z., et al.: Minicpm-v: A gpt-4v level mllm on your phone. arXiv preprint arXiv:2408.01800 (2024)
113. Yim, J., Joo, D., Bae, J., Kim, J.: A gift from knowledge distillation: Fast optimization, network minimization and transfer learning. In: Proceedings of the IEEE conference on computer vision and pattern recognition. pp. 4133–4141 (2017)
114. Yu, T., Zhang, H., Yao, Y., Dang, Y., Chen, D., Lu, X., Cui, G., He, T., Liu, Z., Chua, T.S., et al.: Rlaif-v: Aligning mllms through open-source ai feedback for super gpt-4v trustworthiness. arXiv preprint arXiv:2405.17220 (2024)
115. Yu, W., Yang, Z., Li, L., Wang, J., Lin, K., Liu, Z., Wang, X., Wang, L.: Mm-vet: Evaluating large multimodal models for integrated capabilities. arXiv preprint arXiv:2308.02490 (2023)
116. Yu, W., Yang, Z., Ren, L., Li, L., Wang, J., Lin, K., Lin, C.C., Liu, Z., Wang, L., Wang, X.: Mm-vet v2: A challenging benchmark to evaluate large multimodal models for integrated capabilities. arXiv preprint arXiv:2408.00765 (2024)
117. Yue, X., Ni, Y., Zhang, K., Zheng, T., Liu, R., Zhang, G., Stevens, S., Jiang, D., Ren, W., Sun, Y., et al.: Mmmu: A massive multi-discipline multimodal understanding and reasoning benchmark for expert agi. arXiv preprint arXiv:2311.16502 (2023)
118. Yue, X., Zheng, T., Ni, Y., Wang, Y., Zhang, K., Tong, S., Sun, Y., Yu, B., Zhang, G., Sun, H., et al.: Mmmu-pro: A more robust multi-discipline multimodal understanding benchmark. arXiv preprint arXiv:2409.02813 (2024)
119. Yunxin Li, e.a.: Cognitive visual-language mapper: Advancing multimodal comprehension with enhanced visual knowledge alignment. Proceedings of the 62nd Annual Meeting of the Association for Computational Linguistics (2024)
120. Zagoruyko, S., Komodakis, N.: Paying more attention to attention: Improving the performance of convolutional neural networks via attention transfer. arXiv preprint arXiv:1612.03928 (2016)
121. Zhang, S., Zhang, X., Sun, Z., Chen, Y., Xu, J.: Dual-space knowledge distillation for large language models. arXiv preprint arXiv:2406.17328 (2024)
122. Zhang, Y., Zhang, R., Gu, J., Zhou, Y., Lipka, N., Yang, D., Sun, T.: Llavar: Enhanced visual instruction tuning for text-rich image understanding. arXiv preprint arXiv:2306.17107 (2023)
123. Zhang, Y.F., Wen, Q., Fu, C., Wang, X., Zhang, Z., Wang, L., Jin, R.: Beyond llava-hd: Diving into high-resolution large multimodal models. arXiv preprint arXiv:2406.08487 (2024)
124. Zhu, D., Chen, J., Shen, X., Li, X., Elhoseiny, M.: Minigpt-4: Enhancing vision-language understanding with advanced large language models. arXiv preprint arXiv:2304.10592 (2023)
125. Zong, Z., Ma, B., Shen, D., Song, G., Shao, H., Jiang, D., Li, H., Liu, Y.: Mova: Adapting mixture of vision experts to multimodal context. arXiv preprint arXiv:2404.13046 (2024)

A Token Type Examples

Image

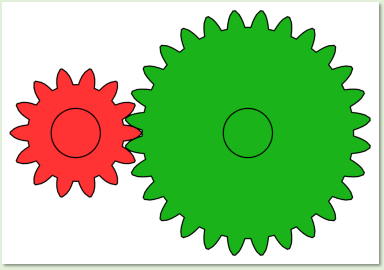

Image Split

Qwen2-VL

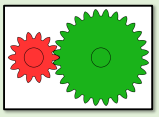

InternVL2, 2.5

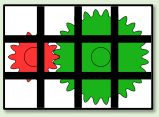

Text

A gear or gearwheel is a rotating machine part typically used to transmit rotational motion and/or torque by means of a series of teeth that engage with compatible teeth of another gear or other part. The teeth can be integral saliences or cavities machined on the part, or separate pegs inserted into it. In the latter case, the gear is usually called a cogwheel. A cog may be one of those pegs or the whole gear. Two or more meshing gears are called a gear train.

InternVL2.5-2B, 8B (InternLM2.5 Tokenizer)

[290, 14586, 607, 14586, 38417, 505, 395, 41101, 5817, 1087, 11287, 1629, 442, 29583, 5902, 1813, 11531, 454, 5304, 40750, 684, 3527, 446, 395, 4169, 446, 17977, 560, 16714, 579, 18294, 17977, 446, 2595, 14586, 607, 1148, 1087, 281, 707, 17977, 777, 517, 25528, 4433, 12126, 607, 55506, 1507, 7983, 1735, 519, 410, 1087, 328, 607, 8784, 30913, 269, 21816, 1263, 563, 281, 890, 410, 15394, 1286, 328, 410, 14586, 505, 6144, 2758, 395, 60179, 38417, 281, 493, 60179, 1377, 517, 959, 446, 1995, 30913, 269, 607, 410, 4521, 14586, 281, 9173, 607, 937, 11447, 418, 52230, 657, 2758, 395, 14586, 5585, 281], **Length: 103**

Qwen2-1B, 7B, 72B | InternVL2.5-1B, 4B, 78B (Qwen2.5 Tokenizer)

[32, 14448, 476, 14448, 38590, 374, 264, 41396, 5662, 949, 11136, 1483, 311, 29282, 91271, 11379, 323, 5144, 41031, 553, 3363, 315, 264, 4013, 315, 17832, 429, 16579, 448, 18146, 17832, 315, 2441, 14448, 476, 1008, 949, 13, 576, 17832, 646, 387, 25098, 4274, 11975, 476, 56609, 1361, 7845, 1589, 389, 279, 949, 11, 476, 8651, 30687, 82, 21578, 1119, 432, 13, 758, 279, 15271, 1142, 11, 279, 14448, 374, 5990, 2598, 264, 61566, 38590, 13, 362, 61566, 1231, 387, 825, 315, 1846, 30687, 82, 476, 279, 4361, 14448, 13, 9043, 476, 803, 11294, 287, 53160, 525, 2598, 264, 14448, 5426, 13], **Length: 102**

InternVL2-76B (Llama-3 Tokenizer)

[32, 14787, 477, 14787, 39690, 374, 264, 42496, 5780, 961, 11383, 1511, 311, 30382, 92371, 11633, 323, 5255, 42131, 555, 3445, 315, 264, 4101, 315, 18311, 430, 16988, 449, 18641, 18311, 315, 2500, 14787, 477, 1023, 961, 13, 578, 18311, 649, 387, 26154, 4371, 12242, 477, 57709, 1385, 8002, 1619, 389, 279, 961, 11, 477, 8821, 31787, 82, 22306, 1139, 433, 13, 763, 279, 15629, 1162, 11, 279, 14787, 374, 6118, 2663, 264, 62666, 39690, 13, 362, 62666, 1253, 387, 832, 315, 1884, 31787, 82, 477, 279, 4459, 14787, 13, 9220, 477, 810, 11546, 287, 54260, 527, 2663, 264, 14787, 5542, 13], **Length: 102**

B Possible Distillation Pair for VLM Combinations: Traditional Distillation versus GenRecal

Student VLM

Teacher VLM: VLM Name (LLM Name)	Qwen2-VL-7B (Qwen2-7B)	Qwen2-VL-2B (Qwen2-7B)	InternVL2.5-8B (InternLM2.5-7B)	InternVL2.5-4B (Qwen2.5-3B)	InternVL2.5-2B (InternLM2.5-1.8B)	InternVL2.5-1B (Qwen2.5-0.5B)
InternVL2-76B (Llama-3-70B)	X	X	X	X	X	X
Qwen2-VL-72B (Qwen2-72B)	O	O	X	X	X	X
InternVL2.5-78B (Qwen2.5-72B)	X	X	X	O	X	O

(a) Traditional Distillation

Student VLM

Teacher VLM: VLM Name (LLM Name)	Qwen2-VL-7B (Qwen2-7B)	Qwen2-VL-2B (Qwen2-7B)	InternVL2.5-8B (InternLM2.5-7B)	InternVL2.5-4B (Qwen2.5-3B)	InternVL2.5-2B (InternLM2.5-1.8B)	InternVL2.5-1B (Qwen2.5-0.5B)
InternVL2-76B (Llama-3-70B)	O	O	O	O	O	O
Qwen2-VL-72B (Qwen2-72B)	O	O	O	O	O	O
InternVL2.5-78B (Qwen2.5-72B)	O	O	O	O	O	O

(b) GenRecal

Fig. 8: We explore the range of distillation combinations between teacher and student VLMs using two approaches: (a) traditional distillation [11] and (b) our proposed model, GenRecal. Unlike traditional distillation—which support only a limited set of pairings—GenRecal offers the flexibility to select any model for distillation, thereby enabling a more versatile and comprehensive distillation framework.

C Extended Related Works

Evolution of Vision-Language Models. Since the emergence of visual instruction tuning [63], there surge many variations of VLMs such as LLaVA-1.5 [61], InstructBLIP [27], ShareGPT-4V [16], MiniGPT-v2 [14] [14, 16, 27, 61, 124], and they initially start with a standard model size of 7B. After that period, numerous VLMs [29, 58, 62, 70] have divided an image into multiple subregions to focus on the image's details so that visual perception is enhanced. CoLLaVO [50] and MoAI [51] utilize computer vision models directly for visual capability, and Mini-Gemini [58], MoVA [125], and Eagle [85] employ multiple vision encoders such as CLIP [78], ConvNext [108], DINO-v2 [75], and SAM [45]. In parallel, Meteor [49] explores the efficient way of learning complex reasoning abilities, and TroL [48] and Phantom [47] investigate propagation modification for how we can embed vision-language knowledge as much as possible despite using the same architectures. More recently, many VLMs like Molmo-72B [28], LLaVA-OneVision-72B [53], NVLM-72B [26], Qwen2-VL-72B [105] and InternVL2.5-78B [20] have employed large-scale language models such as Qwen2/Qwen2.5-72B [111]. Thanks to scaling laws [23, 43], they have closely reached the performances of GPT-4V [74] and Claude-3.5 Sonnet [4]. Therefore, developing VLMs with large-scale language models is getting to a standard these days.

Knowledge Distillation. This provides an effective framework [36] for transferring the rich representations of large, high-performing models to smaller, efficient counterparts while preserving performance. Early studies primarily focused on aligning the output logits of a "teacher" model with those of a "student" [83,100]. Subsequently, the FitNet framework [82] extended this idea by supervising the student using intermediate feature representations rather than final outputs. In this setup, convolutional layers project the student's features to resemble those of the teacher, and discrepancies are minimized using an L2 loss.

Following this feature-based paradigm, later methods explored more sophisticated ways of leveraging internal representations for effective knowledge transfer. For instance, [8,17,92,104] demonstrated that incorporating multiple intermediate layers from the teacher significantly enhances distillation effectiveness. Probabilistic approaches such as PKT [77] reformulated the teacher's knowledge as a probability distribution, aligning it with the student's outputs via KL divergence. Similarly, RKD [76] captured inter-sample relationships, while CRD [96] combined contrastive learning with traditional distillation.

Multi-stage and relational strategies further broadened the field. AT [120] utilized attention maps from several teacher layers, and FSP [113] employed matrices derived from feature maps to guide the student. Later, SP [99] evaluated similarity among input samples, and OFD [35] introduced a margin-based distance metric derived from ReLU activations to capture essential information.

As the methodology matured, two main paradigms emerged. *On-policy* approaches [2,5,34,46] dynamically sample data during training, whereas *off-policy* methods [9, 46, 92, 100, 121] rely on pre-collected datasets. While early research

mostly adopted single-teacher frameworks [2,34,73,86], multi-teacher distillation has gained increasing attention despite challenges such as architectural differences, vocabulary mismatches, and task misalignment [52, 97, 102]. Representative examples include DKMF [103] and FNKD [110], which utilize teacher feature representations, while DGKD [89] aggregates knowledge from multiple teachers to boost student performance.

Recent work has also emphasized refining loss functions used in distillation. MiniLLM [34] and DistiLLM [46] propose modified KL divergences—such as reverse or skewed variants—to reduce overfitting, particularly for long-tail predictions. Similarly, [109] introduced a dynamic loss-balancing scheme that adaptively combines conventional and reverse KL divergences during training. Finally, to enhance reasoning capabilities, recent studies integrate chain-of-thought (CoT) supervision. Methods such as [39, 95] leverage detailed reasoning traces from larger models, while TinyLLM [95] aggregates multi-teacher reasoning to enrich training signals and improve generalization.

D Loss Graphs for Recalibrator

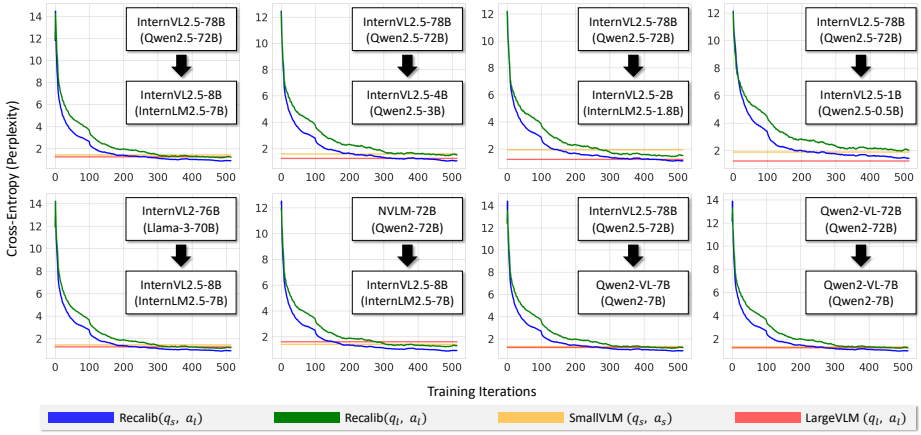

Fig. 9: Illustrating the loss graphs of training Recalibrator, where we deal with various combinations of VLMs: NVLM [26], Qwen2-VL [105], InternVL2 [22], and InternVL2.5 [20]. Note that, the parenthesis in the figure means the name of LLM used in VLMs. 'Recalib(q_s, a_l)' and 'Recalib(q_l, a_l)' represent the cross entropy loss with Recalibrator logits and *VLM-head* of large VLM (see Section 3.2). 'SmallVLM(q_s, a_s)' and 'LargeVLM(q_l, a_l)' means original cross entropy loss for SFT without Recalibrator. They are not used in training Recalibrator. They just represent the averaged cross entropy (perplexity) during the whole training to compare them with 'Recalib(q_s, a_l)' and 'Recalib(q_l, a_l)'.

E Dataset Composition and Analysis

We gather 9M visual instruction tuning dataset covering a wide range of vision-language capabilities such as general visual question answering, dense image captioning, chart/diagram/document understanding, common-sense knowledge, science and math understanding, and multi-dimensional reasoning. Our dataset includes LLaVA-OneVision [53], MMC [60], DenseFusion [57], Cambrian [98], GPT-4V-filtered synthetic data of SA-1B [45] and Infinity-MM [33], Finance-QA [91], Wikipedia knowledge [119], InfoSeek [19], science & mathematical reasoning (SMR) [123], document-downstream/reasoning [40], WildVision [68], SROIE [42], RLAI-F [114], M3CoT [18], LLaVAR [122], KonIQ [38], iNaturalist2018 [101]. For further analysis, we particularly categorize the visual instruction tuning dataset that we use to build GenRecal into three domains: 'Knowledge', 'Science & Math', and 'Chart & Document'. Based on these categories, we conduct dataset composition analysis by removing each of the three domains. This implies that MMMU [117] requires VLMs' ability for the domain of 'Knowledge' more than the others, while MathVista [66] requires their capabilities for 'Science & Math'.

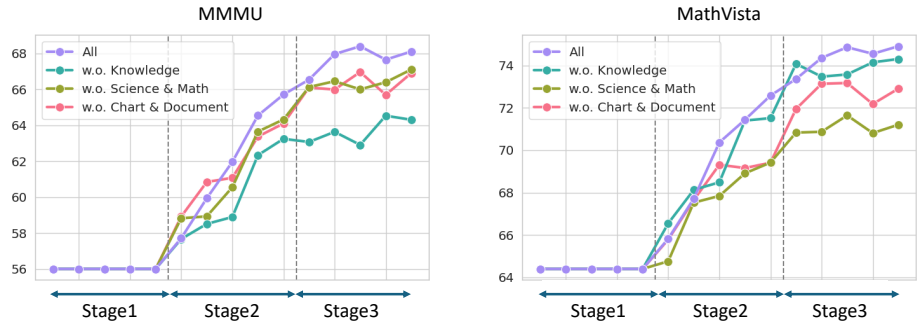

Fig. 10: Accuracy trends across different datasets: (Left) MMMU [117], and (Right) MathVista [66] over three training stages. The performance is shown for different category of visual instruction tuning dataset: "All" (without any exclusion), "w.o. Knowledge", "w.o. Science & Math", and "w.o. Chart & Document". The results indicate the impact of these exclusions on accuracy progression, highlighting how the absence of specific knowledge domains affects. Note that, Note that each data point within the same stage represents 20% of the training progress, with five data points measured per stage.

- **Knowledge**: GPT-4V filtered synthetic of SA-1B [45] and Infinity-MM [33], Wikipedia Knowledge [119], Wild-Vision, InfoSeek [19], WildVision [68], and iNaturalist2018 [101]
- **Science & Math**: LLaVA-OneVision (subset) [53], Cambrian (subset) [98], Finance-QA [91], SMR [123], M3CoT [18], and KonIQ [38]
- **Chart & Document**: LLaVA-OneVision (subset) [53], Cambrian (subset) [98], MMC [60], RLAI-F [114], document-downstream/reasoning [40], SROIE [42], and LLAVAR [122]